RSC Advances

ROYAL SOCIETY OF CHEMISTRY

www.rsc.org/advances

graphical abstract

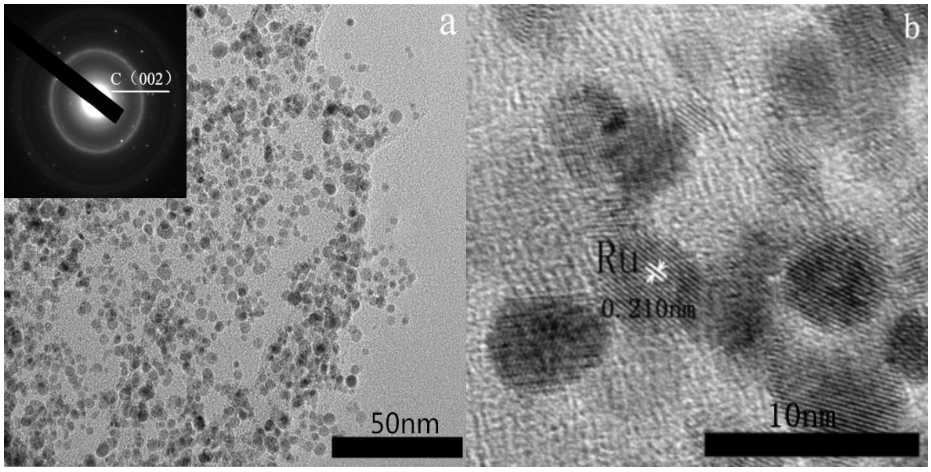

The ruthenium particles with an average size of 3.17 nm are uniformly anchored on supercritical water-reduced graphene oxide (WRG).

One-step green synthesis of a ruthenium/graphene composite as a highly efficient catalyst

Jian Zhao,*[a,b,c] Wenbin Hu,[a] Hongqi Li,[a] Min Ji,[a] Changzhi Zhao,*[a] Zhaobo Wang,[a] Haiqing Hu[a]

[a]*Key Laboratory of Rubber-Plastics Ministry of Education/Shandong Provincial Key Laboratory of Rubber-Plastics, Qingdao University of Science & Technology, No. 53 Zhengzhou Road, Qingdao 266042, China*

[b]*Shanghai East Hospital, the Institute for Biomedical Engineering and Nanoscience, Tongji University School of Medicine, Tongji University, No.1239 Siping Road, Shanghai, 200092, China*

[c]*The Materials Science and Engineering Program, Department of Mechanical and Materials Engineering, College of Engineering and Applied Science, University of Cincinnati, 2600 Clifton Ave., Cincinnati, Ohio，45221, USA*

*Corresponding author: Fax: +86 0532 84022725; Tel: +86 0532 84023847;

E-mail: zhaojian@gmail.com (J. Zhao)

Abstract

A simple, rapid, and green one-step synthesis was developed for an efficient catalytic composite by simultaneously reducing graphene oxide sheets and ruthenium ions in supercritical water without any external reducing and stabilizing agents. No organic solvent was involved in the entire synthesis process. X-ray diffraction，transmission electron microscopy, X-ray photoelectron spectroscopy and gas chromatography were used to characterize the nanohybrid material and its activities for hydrogenation of benzene and cyclohexene, respectively. The metallic ruthenium particles with an average size of 3.17 nm and narrow size distribution were uniformly anchored on supercritical water-reduced graphene oxide (WRG). High metal nanoparticle content (43.6 wt%) on WRG was mainly ascribed to the special role of supercritical water. The as-synthesized nanohybrid (Ru/WRG) exhibited high catalytic activities, attributable to fine dispersion of the Ru nanoparticles and their intimate interfacial contact with the carbon support. The Ru/WRG composite was reused five times for hydrogenation of cyclohexene without detectable loss of activity, a result of its stable structure. In principle, the unique supercritical method is extendable to support other metal nanoparticles to fabricate highly efficient nano-catalysts.

1. Introduction

Graphene，a two-dimensional (2D) material, is structured with a single-atom thick sheet of hexagonally arrayed sp^2-bonded carbon atoms. This unusual nanostructure is ideal for constructing of a carrier of metal and/or metal oxide nanoparticles. Other advantages of graphene include large surface area, strong mechanical strength, high thermal conductivity, superb electron mobility, and chemical inertness with open structure of both sides.[1-3] Graphene-based hybrids have shown promising applications in capacitors, fuel cells, catalysis, hydrogen storage, and sensors. [2, 4-8]

The methods of preparing graphene mainly include mechanical exfoliation, thermal expansion, epitaxial growth, chemical vapor deposition[2], reduction of graphite oxide (GO) ,[9-12] unzipping of carbon nanotubes ,[13, 14] and direct exfoliation of pristine graphite.[15-17] The chemical route of making graphene has been a popular approach owing to its scalability in production and economical cheapness.[1, 18] In fabrication of graphene-based metal hybrids, graphite oxide was generally employed as the starting material for its richness in various functional groups. Graphite oxide is often formed during oxidation of graphite, which facilitates its dissolution in several solvents, especially in water (forming graphene oxide)[19], and allows for intercalation of metal precursors into the interlayers of GO for nucleation and growth of the metal nanoparticles.[20]

Ruthenium is a transition metal, widely used as catalyst for carbon monoxide oxidation[21], ammonia synthesis[22], electrocatalysis[23], ammonia decomposition[24],

hydrogen storage,[25] and hydrogenation of aromatics[26]. However, Ru particles are often found to aggregate after reaction, leading to low catalytic activity after extended use. To address this problem, inorganic and organic materials were employed as carriers to support Ru nanoparticles. [22, 24, 27, 28]

Although graphene can be an excellent support for metal nanoparticles, a few successful methods were reported on fabricating Ru/graphene composites (despite the fact that the growth of graphene on Ru was extensively studied). Jung et al. reported a synthesis of ruthenium-based nanomaterials, supported on reduced graphene oxide (rGO), by a modified polyol method using $NaBH_4$ as a reducing agent.[29] The hybrid efficiently functioned as air cathodes in non-aqueous electrolyte Li-air cells. Cao et al. developed a one-step chemical co-reducing route for preparation of graphene-supported Ru nanoparticles for hydrolytic dehydrogenation of ammonia borane using methylamine borane as reducing agent and GO as starting materials.[30] As a result of low Ru concentration and poor crystallinity, no well-defined diffraction peaks were observed in XRD. Thermal reductions of metal doped-GO precursors were carried out in nitrogen and hydrogen atmospheres.[23] The Ru concentration in the Ru/graphene hybrid was as low as 0.5 wt %. In order to achieve efficient stabilization of Ru nanoparticles, ionic liquids were utilized as a medium to generate graphene-supported metal composites for their excellent solvent and surfactant-like properties. Janiak et al. investigated an functional ionic liquid-assisted immobilization of Ru on thermally reduced graphene by decomposition of its metal carbonyl precursor under microwave irradiation.[31] The resulting composites with a Ru content

of 15 wt% were active hydrogenation catalysts. Liu et al. reported on the exfoliation of graphite into graphene sheets with an ionic liquid and obtained 5 wt% Ru in the composite. [32]

Recent works on first-principles based calculations predicted pristine graphene to be not suitable for direct supporting of the Ru metal nanoparticles owing to its low surface energy and chemical inertness.[33] Further experimental investigation on Ru/graphene catalysts indicated negligible Ru content on defect-free graphene, while it reached a metal loading of 3.4 wt%on reduced graphene oxide surface.[20] Most of Ru nanoparticles were found to be reduced in solvent and not efficiently loaded on the reduced graphene oxide. So far, only few studies were reported on the rapid synthesis by which mass loading of Ru was possible on the graphene surface. In view of the fact that the reducing agents reported in literature are toxic or the preparation processes are often time-consuming, it is highly desirable to explore the possibility of a simple and green chemistry route for the production of Ru/graphene hybrids.

Supercritical water (SCW), a green chemistry alternative to organic solvents, can act as a reducing agent.[25] Its physiochemical properties can be easily controlled by adjusting pressure and temperature. Supercritical water behaves as a water-like fluid with strong electrolytic solvent power, extremely low surface tension, and high diffusion coefficient.[34] The dielectric constant of supercritical water can reach those of organic solvents. These properties make it an excellent solvent for the synthesis of nanomaterials. [34-36] Other supercritical fluids were also used for the synthesis of metal nanoparticles supported by carbon substrate.[36-38] Unfortunately, they are not

applicable to GO or pristine graphene either because of low reducing power of the supercritical systems for GO or due to the fact that the carbon sheets are not stable in the fluids and can be easily aggregated into layered structure. In the latter case, the accessible surface area of graphene or GO sheets is significantly lowered, leading to unfavorable agglomeration of metal particles.

In this work, highly dispersed ruthenium/graphene nanocomposite was developed in supercritical water using graphene oxide as a starting material and $RuCl_3$ the precursor. Several advantages in this unique method include: (1) water medium (no organic solvent was involved in the entire synthesis process); (2) no organic or toxic reducing and stabilizing agents; (3) high loading of Ru in comparison with those reported in literature, and the metal content is adjustable by simply changing the weight ratio of $RuCl_3$ to GO, and (4) rapid reaction in a single step. To the best of our knowledge, there has been no report on a single step, in situ, and green synthesis of metal/graphene nanohybrids using supercritical water. The Ru/supercritical water-reduced graphene oxide (Ru/WRG) hybrid showed excellent performance in hydrogenation of benzene and cyclohexene. The special effect of supercritical water, in conjunction with dense defects and oxygen-containing functional groups on the carbon support, was found to play an important role in high loading and fine dispersion of the Ru nanoparticles.

2. Experimental Section

2.1. Materials

Natural graphite flakes were obtained from Qingdao Ruisheng Graphite Co.Ltd.

(purity 99.99%, particle size 40 μm). Ruthenium chloride anhydrous ($RuCl_3$) was purchased from Sinopharm Chemical Reagent Co. Ltd. Acetone, cyclohexene, and benzene were of analytical grade. Double-distilled water was used in the experiments. The commercial Ru/C catalyst was purchased from Baoji Ruike Co., Ltd., China. GO and activated carbon (JCAC-1800) were obtained from Nanjing XFNANO Materials TECH Co., Ltd, China.[39, 40] All glassware and Teflon coated magnetic stir bars were cleaned with acetone, followed by copious rinsing with water before drying in an oven at 100 °C.

2.2. Synthesis of Ru/WRG composite

In a typical experiment, 20 mg of GO was dispersed in 10mL of water after sonication (100W) for 2h, forming stable graphene oxide colloid. 40 mg of $RuCl_3$ (the weight ratio of $RuCl_3$ to GO was 2:1) was then added to the colloid, followed by stirring for 1h. Subsequently, the suspension was loaded into a stainless steel autoclave. After flushing with nitrogen gas for 10 min, the autoclave was sealed and maintained at the desired temperature (400 °C) and pressure (23.5 MPa) for 2h. The autoclave was cooled to room temperature naturally. The dark precipitate was washed with water and vacuum-dried at 60 °C for 48h, and maintained in a nitrogen atmosphere. A sample in the absence of GO was prepared under similar conditions.

2.3. Characterization

XRD patterns were obtained using a D-MAX 2500/PC operated at 40 kV and 100 mA with Cu Kα radiation (λ=0.15418 nm). The morphologies of the samples were studied by TEM on a JEOL 2010 TEM, equipped with an EDS. The particle size

distribution was determined by counting over 100 particles using the Nano Measurer 1.2 software. TEM samples were prepared by depositing droplets of hybrid-methanol suspension on copper grids coated with lacey carbon film. The resulting composites were analyzed by inductively coupled plasma spectroscopy/optical emission spectroscopy (ICP/OES, Perkin-Elmer, Optima 3300XL with AS 91 autosampler) for metal content. The XPS characterization of the composite was performed on a RBD upgraded PHI-5000C ESCA system (Perkin Elmer) with Al Kα radiation (hν=1486.6 eV) and the data analysis was carried out using XPSPEAK 41 software. The C1s peak position was set to 284.6 eV and taken as an internal standard.

2.4. Measurement of catalytic activities

The catalytic properties of the Ru catalyst (the initial weight ratio of $RuCl_3$ to GO was 2:1）for hydrogenation of benzene and cyclohexene were evaluated using a 50 mL stainless-steel batch reactor, which was equipped with glass inlays to eliminate any catalytic influence of the metal surface in reactions. A suitable amount of Ru catalyst and 4 mL of benzene or cyclohexene was placed in the reactor. Subsequently, the reactor was purged with high purity H_2 (＞99.99％) 5 times to remove air inside. Next, a reaction pressure was generated at the desired reaction temperature (60 °C) and the reaction system was magnetically stirred at a speed of 300rpm. The H_2 pressure was kept constant by replenishing H_2 in the reaction. The system was maintained at constant condition during the entire reaction process. After reaction, the reactor was cooled to room temperature in an ice-water bath and the pressure in the reactor was released. To investigate recyclability of the catalyst, the isolated Ru catalyst was

filtered after reaction (for hydrogenation of cyclohexene) and reused by adding fresh cyclohexene in the next hydrogenation run. The hydrogenation products were analyzed by gas chromatography (GC) (Agilent 6820) with a PEG-20M capillary column (0.25 mm in diameter, 30 m in length) and a flame ionization detector (FID).

3. Results and discussion

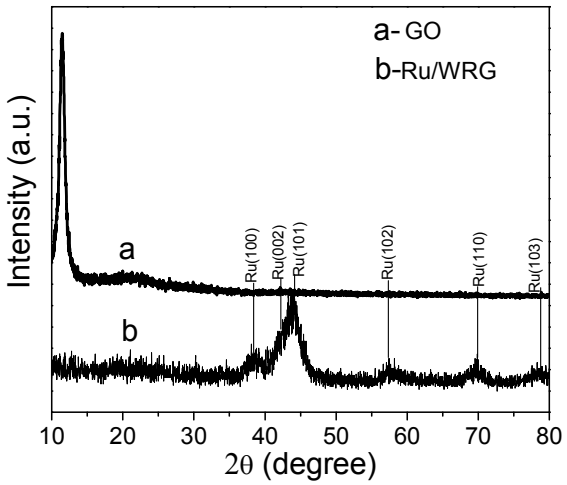

Fig.1. XRD patterns of GO and Ru/WRG (the weight ratio of $RuCl_3$ to GO was 2:1）

The XRD patterns of the GO and Ru/WRG are shown in Figure 1. The characteristic diffraction peak at 2θ=11.1° (002 reflection) (Fig. 1a) for the GO sample corresponds to a spacing of 0.80 nm in the stacking structures due to the introduction of oxygenated functional groups. This intense peak disappears and no peak associated with graphite-like structure is found in the XRD pattern of the Ru/WRG nanocomposite (Fig. 1b). This indicates the inhibition of graphene aggregation by the attached nanoparticles during the fabrication of the composite. The diffraction peaks at 38. 5° (100); 42.2° (002); 44.0° (101); 57.4° (102); 69.6° (110), and 78.2° (103) can be well indexed to a typical hexagonal phase of Ru (JCPDS Card

NO 60663). The broad signals reflect small mean crystallite sizes in Ru/WRG. No diffraction peaks associated with separated phase of Ru oxides was detected in the Ru/WRG composite based on XRD, indicating that the metal oxide phases might be present only in a small amount or in amorphous forms in the composite. The XRD analysis clearly shows the formation of Ru in the supercritical water-assisted process.

Figure 2 (a) shows the TEM images of the Ru/WRG composite. The Ru metal nanoparticles are uniformly and densely distributed on nearly transparent graphene sheets with little aggregation. The deposited particles remain strongly immobilized on the graphene sheets, despite of intense sonication for several hours. The attached Ru nanoparticles can prevent the reduced GO from aggregation and restacking. The HRTEM inspection (Fig. 2b) shows the crystalline nature of the nanoparticles. Aligned crystal lattices, with an average spacing of about 0.210 nm, correspond to the (101) plane of Ru. Fig. 2b also shows the small contact angle between WRG and the Ru nanoparticles. That is, the contact area between WRG and the Ru nanoparticle is large, implying strong WRG-Ru interaction. This can partly explain why the nanoparticles are firmly anchored on WRG despite prolonged sonication. Presented as an inset in Fig 2a, the corresponding selected area electron diffraction (SAED) pattern displays characteristic Ru diffraction circles. These diffraction patterns do not show clear spots, but concentric rings. Each ring consists of a large number of small spots, an indication of fine crystallites. In addition to these circles, diffraction patterns from hexagonal graphene structure reflections are also observed.[31,15] The average size of the Ru nanoparticles is 3.17 nm within the size range of 1.5-5.5 nm (Fig. 2c). Energy

dispersive spectrometer (EDS) analysis confirms the Ru element without Cl (Fig. 2d). Small amount of Fe, Cr and Cu elements was detected, indicating corrosion of the stainless steel autoclave by supercritical water.

The hybrid was analyzed for exact amount of the metal by using inductively coupled plasma/optical emission spectroscopy (ICP/OES). The Ru loading is found to be 43.6 wt％ in Ru/WRG, much higher than those of graphene-based Ru composites reported in literature. Actually, the theoretical loading of Ru is estimated to be about 50 wt% assuming that all the Ru was immobilized on WRG. That is, not much Ru was left in solution. As Ru is a noble metal, its high utilization is crucial. In many cases, low loading of Ru implies that a large portion of Ru species are left in solution instead of on carbon supports. The high loading of Ru is also very useful for practical applications in industry since it greatly reduce the volume or mass of industrial products (Ru is the active species whereas graphene is inert). To avoid the corrosion problem in the stainless steel autoclave, we performed the same experiment.using a special alloy autoclave that is suitable for supercritical water. The Ru loading（45.7 wt%）of the resulting Ru/graphene hybrid do not show significant difference from the original composite. The elements Fe, Cr and Cu were not found any more. Interestingly, we also find that the loading of Ru nanoparticles on WRG can be controlled by simply changing the weight ratio of $RuCl_3$ to GO (Fig. S1, see Supporting Information).

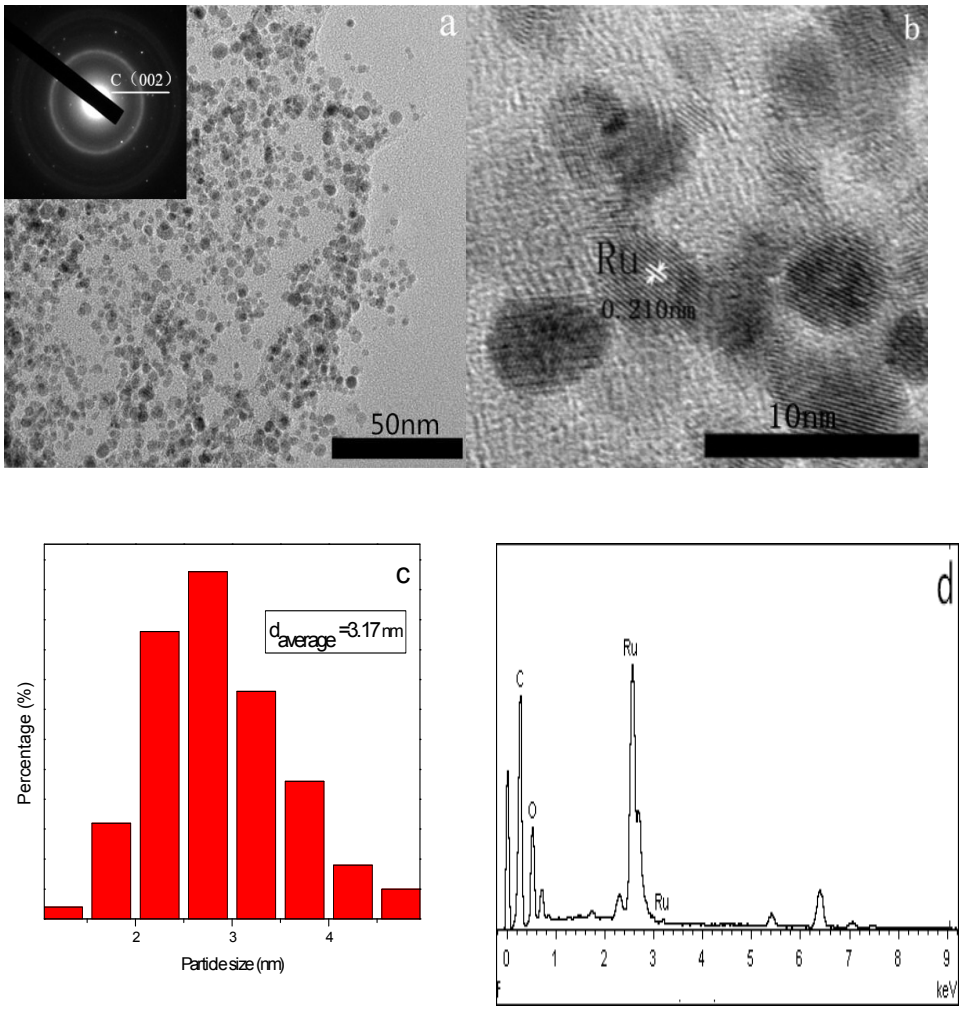

Fig.2. (a) TEM image of Ru/WRG with SAED pattern as an inset (at an initial weight ratio of $RuCl_3$ to GO of 2:1); (b) HRTEM image of Ru/WRG; (c) nanoparticle size distribution of Ru/WRG, and (d) EDS spectrum of Ru/WRG.

GO is heavily oxygenated graphene bearing hydroxyl and epoxide functional groups on its basal plane, in addition to carbonyl and carboxyl groups located at the sheet edge. These oxygen-containing functionalities can stabilize the dispersion of the GO sheets in water and result in their exfoliation into a few single layers.[4] Recently, it has been demonstrated that supercritical water could act as a reducing agent for GO under hydrothermal conditions, representing a new and green route for the production of graphene.[34] In acid media, GO sheets or reduced GO (RGO) sheets tend to

aggregate due to protonation of negatively charged O^- and COO^- groups on the carbon surface. The electrostatic repulsion between the sheets of GO or RGO is not strong enough to overcome the stacking of the carbon sheets by noncovalent interactions such as π-π interactions or hydrogen-bonding.[34]

In our experiments, upon adding ruthenium chloride, some of Ru^{+3} cations could be adsorbed onto GO surfaces through electrostatic interactions of the oxygen-containing functional groups. It was found that the pH value of the GO solution changed to 2.7 from 6.3 upon addition of $RuCl_3$. This would be a much more acid environment in which the GO colloid or its reduced product became unstable.[35] In our case, however, the presence of Ru ions or the resulting Ru nanoparticles on the carbon support was capable of stabilizing the system, avoiding unfavorable aggregation of the carbon sheets.

As is well known, in its supercritical state, water exhibits unique properties such as near-zero surface tension, low viscosity, high diffusion, and strong electrolytic solvent power. The hydrogen bonding between the GO sheets and water can largely break from ambient to supercritical environments. These features facilitate the loading of Ru species on the carbon sheets. By exploiting the reducing effect inherent to supercritical water, the WRG-based composites were developed by in situ combination with mass loading of metal Ru nanoparticles.

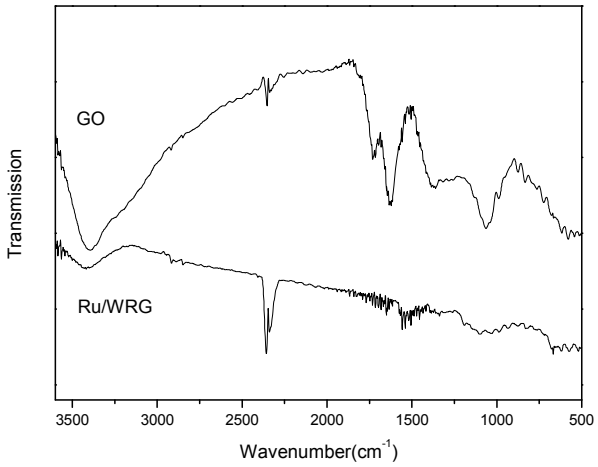

Fig.3. FT-IR spectra of GO and Ru/WRG.

Figure 3 shows the FTIR spectra of GO and Ru/WRG. It can be seen clearly that the intense absorption peak (-OH, stretching vibration mode） at 3395 cm^{-1}, C=O peak at 1732 cm^{-1}, and C-O peak at 1065 cm^{-1} of GO are significantly decreased after the formation of the Ru/WRG hybrid. This is a clear indication of GO reduction to graphene during the preparation process.

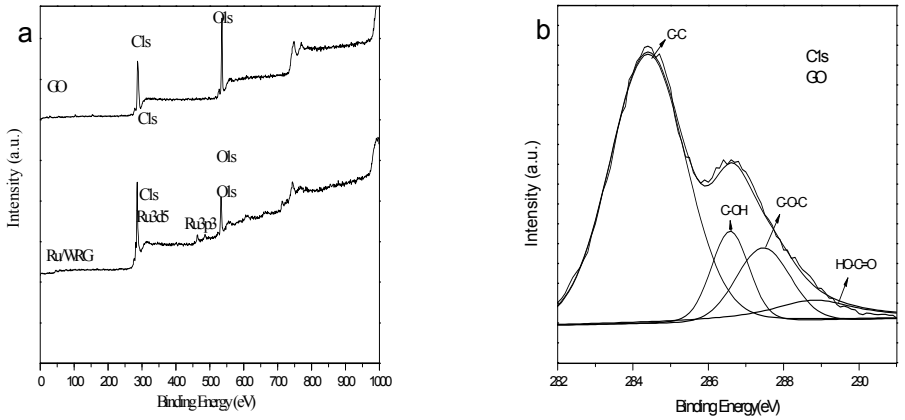

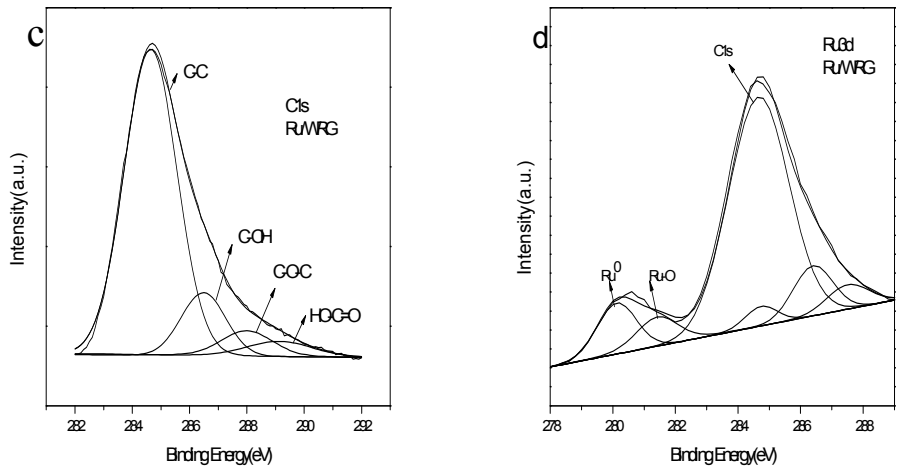

Fig.4. (a) XPS survey spectra of GO and Ru/WRG; (b) C 1s XPS spectrum of GO; (c) C 1s XPS spectrum of Ru/WRG, and (d) Ru 3d XPS spectrum of Ru/WRG.

XPS was used to probe the chemical valence state of Ru and GO before and after the supercritical water treatment. The binding energies obtained in the XPS analysis were corrected for specimen charging by referencing the C 1s peak to 284.6 eV. As shown in Figure 4a, the survey XPS pattern of Ru/WRG (the survey XPS pattern of GO is also shown) indicates the coexistence of C, Ru, and O in the hybrid. No Cl is detectable, suggesting its high purity without the presence of the metal precursor. Compared with the peaks of GO (Fig. 4b), the intensities of the –C-OH (286.6 eV), -C-O-C- (287.4 eV), and –COOH (288.8 eV) groups in the C 1s XPS spectrum of Ru/WRG (Fig. 4c) significantly decrease, indicating deoxygenation of GO. Although the Ru 3d signal is somewhat obscured by C 1s of the carbon substrate, the deconvoluted spectrum (Fig. 4d) presents a doublet for two chemically different Ru entities with peak binding energies of 280.1 (Ru $3d_{5/2}$) and 284.7 eV (Ru $3d_{3/2}$). These results confirm the presence of Ru^0 in the composite.[41] The peak at 281.3 eV can be

ascribed to a Ru-O component, likely resulting from the bond between the oxygen-containing groups of WRG with Ru.[42] The Ru species and some of the functional groups on GO were simultaneously reduced by supercritical water, thereby forming small Ru nanopartciles that were uniformly and strongly anchored on the WRG surface.

The catalytic activity of the composite was analyzed using the benzene and cyclohexene hydrogenation as the model reactions and the results are listed in Table 1. The reactions were performed at 60 °C under H_2 atmosphere with a cyclohexene or benzene to Ru molar ratio of 5.0×10^3, where cyclohexene and benzene act as both reactant and solvent. The catalyst can be well dispersed in cyclohexene or benzene without any additional solvents. It can also be easily separated from the final products. The Ru/WRG catalyst converted cyclohexene almost completely into cyclohexane within 0.5 hr at 60 °C and H_2 pressure of 2 MPa. The turnover frequency (TOF) reached 1.0×10^4 h^{-1} (Table 1, entry 1). The hydrogenation of benzene catalyzed by Ru/WRG was also investigated (Table 1, entries 6-8). Benzene could be hydrogenated to cyclohexane with essentially complete conversion at 60 °C for 2h, under H_2 pressure of 6 MPa (entry 8). The TOF reached 2475 h^{-1}, indicating that the Ru/graphene catalyst is very active for hydrogenation reactions compared with other nanocatalysts.[42-44] As the weight ratio of $RuCl_3$ to GO was decreased to 1:1, the TOF for benzene hydrogenation (at a temperature of 60 °C, 1h and H_2 pressure of 6 MPa) is 4100 h^{-1}, showing no significant difference as compared with the Ru/WRG sample at the weight ratio of $RuCl_3$ to GO of 2:1 (entry 7). For comparison, benzene

hydrogenation was carried out with the commercial Ru/C catalyst (entry 9). The as-prepared Ru/WRG was found much more active than the commercial Ru/C. We note that when metallic ruthenium was loaded on activated carbon under the same preparation conditions, the average particle size of Ru particles was found to be about 10 nm with a dominant fraction of Ru particles larger than 5 nm (see Fig. S2, Supporting Information). The homemade Ru/AC composite (entry 10) is also much less active than the as-prepared Ru/WRG.

Table 1. The hydrogenation reactions catalyzed by the Ru/WRG composite (the weight ratio of $RuCl_3$ to GO is 2:1） and commercial Ru/C catalyst.

Entry	Catalyst	Substrate	T/℃	P_{H2}/Mpa	t/h	Yield/%	TOF/ h^{-1}
1	Ru/WRG	Cyclohexene	60	2	0.5	>99	$>9.9\times10^3$
2	Ru/WRG	Cyclohexene	60	2	0.5	>99	$>9.9\times10^3$
3	Ru/WRG	Cyclohexene	60	2	0.5	>99	$>9.9\times10^3$
4	Ru/WRG	Cyclohexene	60	2	0.5	>99	$>9.9\times10^3$
5	Ru/WRG	Cyclohexene	60	2	0.5	>99	$>9.9\times10^3$
6	Ru/WRG	Benzene	60	2	1	68	3400
7	Ru/WRG	Benzene	60	6	1	79	3950
8	Ru/WRG	Benzene	60	6	2	>99	2475
9	commercial Ru/C	Benzene	60	6	7	92	657
10	homemade Ru/AC	Benzene	60	6	7	86	614

Reaction conditions: substrate/Ru (mol/mol) = 5000, reaction temperature: 60 ℃. Analysis: GC (Agilent 6820) is equipped with a flame ionization detector (FID) and a PEG-20M capillary column (0.25 mm in diameter, 30 m in length). Turnover frequency (TOF) = mol of product (cyclohexane) · $(\text{mol of Ru})^{-1}$ · h^{-1}.

The stability of the composites was investigated by taking the cyclohexene hydrogenation as an example. Upon reusing the catalyst five times for reaction, no activity loss was observed (even at very high conversion; Table 1, entries 1-5), indicating high stability of the as-prepared catalyst. After 5 cycles of catalysis, the Ru

loading is 42.9 wt%. The recovered catalyst after the fifth run durability test was examined by TEM. It is shown that the metal particles remain firmly anchored on WRG with insignificant aggregation (Fig. 5 a and b). The metal particle size (Fig. 5 c) after five runs is almost identical to the fresh sample. The high activity and stability of the catalyst indicates strong interaction between the particles and graphene, consistent with the TEM observation. The high performance of the catalyst is associated with its optimum structures, in which the fine metal particles are strongly immobilized on the graphene sheets with monodispersibility in supercritical water.

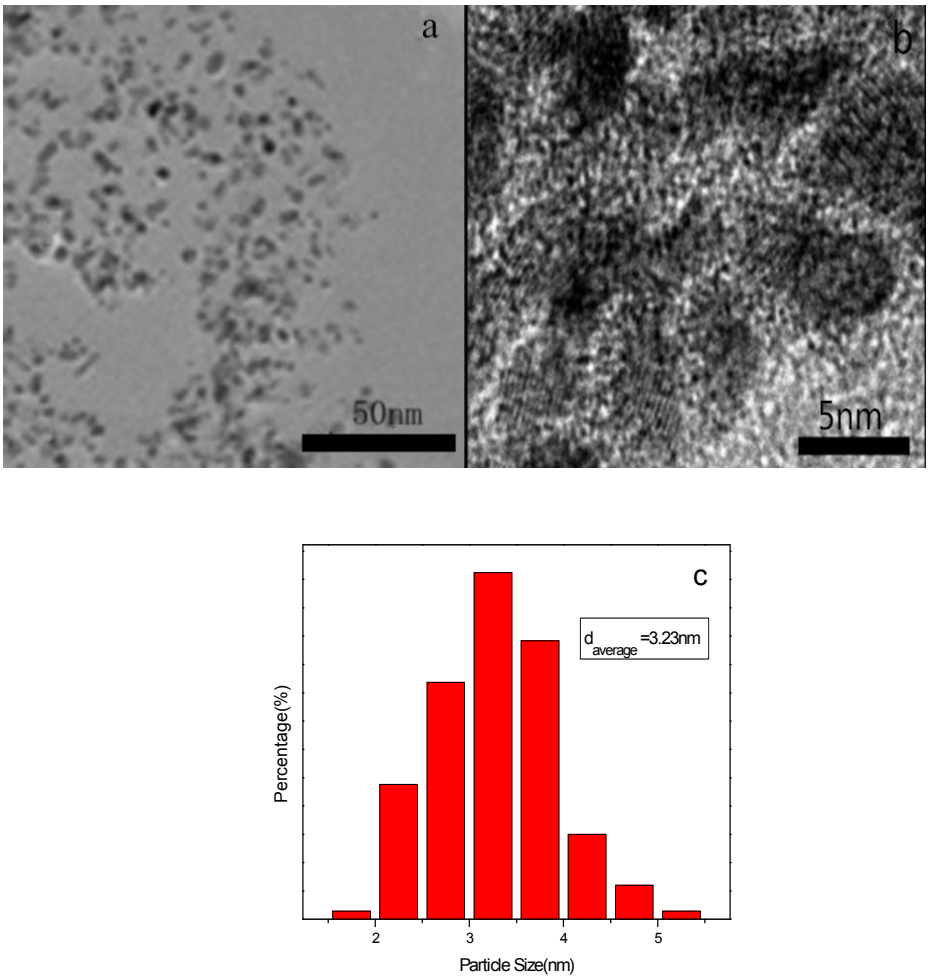

Fig. 5. (a) (b) TEM images and (c) particle size distribution of Ru/WRG, after five consecutive catalytic hydrogenation runs of cyclohexene (after entry 5 of Table 1).

All experimental results from XRD, TEM, EDS and XPS analysis have shown formation of Ru^0 on WRG in supercritical water. It is difficult to give an exact mechanism for the reduction of the Ru^{3+}. Zhao el al. reported on thermal reduction of Ru ions to Ru^0 by carbon species at high temperatures (900° C).[45] In this study, one might believe that the supercritical fluid significantly lowered the decomposition temperature of Ru species simply due to a more reactive environment inherent to supercritical water. In the absence of GO, however, very large Ru agglomerates consisting of particles with a mean size of about 10 nm (Fig. 6) were formed in supercritical water, implying that the robust reducing power of supercritical water may also play a large role. Hence, the Ru^0 might be produced by two routes simultaneously. The WRG sheets behaved as templates where high dispersion and good crystallinity of Ru nanoparticles were anchored. It was reported that carbon nanotubes could be thinned in supercritical water.[46] In this study, the consumption of the carbon support during the Ru reduction in supercritical water resulted in intimate Ru-carbon point contacts and thus formed a "surface-contact" on WRG, as shown in Fig. 2b.[47-49] This intensive contact between the Ru metal and the carbon substrate (Ru-carbon) as well as enhanced hydrogen spillover effect, could partly explain the excellent catalytic performance of the Ru/WRG.[47-49]

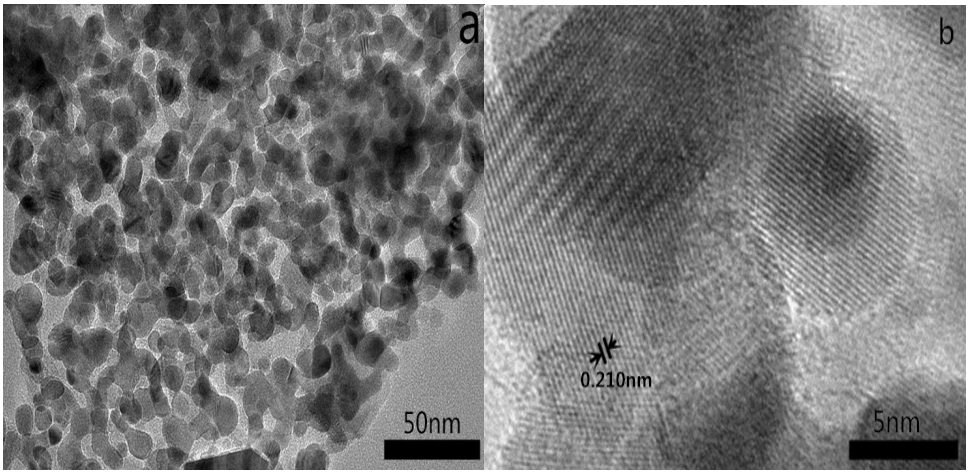

Fig.6. TEM images of Ru particles prepared in the absence of GO

Recent theoretical calculation and experimental results revealed that the use of defective graphene as a support would improve the stability of Ru nanoparticles and promote the adsorption of benzene and hydrogen molecules due to the hybridization between the dsp states of Ru particles and the sp^2 dangling bonds at defect sites.[33] It is consistent with high stability and superior catalytic performance of benzene hydrogenation in the Ru/defective-graphene composites.[33] Supercritical fluids exhibit unusual behaviors such as low viscosity, rapid diffusivity, and absence of surface tension. These unique properties significantly facilitate the transfer of reactants onto complicated surfaces, resulting in complete wetting of the carbon sheets with the Ru species in supercritical water. It is also well known that numerous framework defects and small defective graphene fragments remain on graphene surface upon reduction.[50] It turned out that the Ru nanoparticles produced from the reduction of $RuCl_3$ preferably deposited on the WRG surface instead of in solution, which was capable of stabilizing Ru nanoparticles through the interactions with defects and oxygen functional groups.[51] Namely, by taking advantage of the special role of supercritical

water, the metal nanoparticles can be anchored more efficiently and strongly on graphene. The combination of high particle dispersion and the intimate interfacial contact between Ru and the carbon support is responsible for high activity and stability of the Ru/WRG.

4. Conclusions

In summary, we have successfully fabricated a Ru/graphene nanocomposite using a simple, clean and rapid supercritical fluid route. The "water-only" strategy has shown great advantages in removing oxygen functional groups from graphene oxide, converting Ru ion to Ru^0, and strengthening the Ru-support interaction. The metal particles are uniformly distributed on the water-reduced graphene oxide with an average size of 3.17 nm and narrow size distribution. Supercritical water has been shown in this study as an ideal medium and reducing agent that greatly facilitates particle deposition on the reduced graphene oxide at high loading. The composite exhibits excellent catalytic performance for hydrogenation of benzene and cyclohexene, which is associated with the strong interaction between highly dispersed ruthenium nanoparticles and the supporting substrate. The supercritical method can be used to the synthesis of other graphene-based metal nanoparticles.

Acknowledgements

The work was funded by the National Natural Science Foundation of China (nos. 51373088 and 51073082) and State Key Laboratory of Molecular Engineering of

Polymers (open project K2013-20, Fudan University). We thank Jian Yu at Institute of Chemistry, CAS for allowing us to use his special alloy autoclave.

References

1. V. Singh, D. Joung, L. Zhai, S. Das, S. I. Khondaker and S. Seal, *Progress in Materials Science*, 2011, **56**, 1178-1271.

2. H. Wang and H. Dai, *Chemical Society Reviews*, 2013, **42**, 3088-3113.

3. Y. Si and E. T. Samulski, *Chemistry of Materials*, 2008, **20**, 6792-6797.

4. J.-Y. Kim, K.-H. Kim, S.-B. Yoon, H.-K. Kim, S.-H. Park and K.-B. Kim, *Nanoscale*, 2013, **5**, 6804-6811.

5. G. Zhou, D.-W. Wang, L.-C. Yin, N. Li, F. Li and H.-M. Cheng, *ACS Nano*, 2012, **6**, 3214-3223.

6. X. Liu, C. Meng and Y. Han, *Nanoscale*, 2012, **4**, 2288-2295.

7. G. Goncalves, P. A. A. P. Marques, C. M. Granadeiro, H. I. S. Nogueira, M. K. Singh and J. Grácio, *Chemistry of Materials*, 2009, **21**, 4796-4802.

8. B. Sun, Z. Jiang, D. Fang, K. Xu, Y. Pei, S. Yan, M. Qiao, K. Fan and B. Zong, *ChemCatChem*, 2013, **5**, 714-719.

9. T. Kim, H. C. Kang, T. T. Tung, J. D. Lee, H. Kim, W. S. Yang, H. G. Yoon and K. S. Suh, *RSC Advances*, 2012, **2**, 8808-8812.

10. P. Kumar, B. Das, B. Chitara, K. Subrahmanyam, K. Gopalakrishnan, S. Krupanidhi and C. Rao, *Macromolecular Chemistry and Physics*, 2012, **213**, 1146-1163.

11. P. Kumar, K. Subrahmanyam and C. Rao, *Materials Express*, 2011, **1**, 252-256.

12. P. Kumar, K. Subrahmanyam and C. Rao, *International Journal of Nanoscience*, 2011, **10**, 559-566.

13. D. V. Kosynkin, A. L. Higginbotham, A. Sinitskii, J. R. Lomeda, A. Dimiev, B. K. Price and J. M. Tour, *Nature*, 2009, **458**, 872-876.

14. P. Kumar, L. Panchakarla and C. Rao, *Nanoscale*, 2011, **3**, 2127-2129.

15. Y. Hernandez, V. Nicolosi, M. Lotya, F. M. Blighe, Z. Sun, S. De, I. McGovern, B. Holland, M. Byrne and Y. K. Gun'Ko, *Nature Nanotechnology*, 2008, **3**, 563-568.

16. P. Kumar, *RSC Advances*, 2013, **3**, 11987-12002.

17. U. Maitra, H. Matte, P. Kumar and C. Rao, *CHIMIA International Journal for Chemistry*, 2012, **66**, 941-948.

18. D. R. Dreyer, S. Park, C. W. Bielawski and R. S. Ruoff, *Chemical Society Reviews*, 2010, **39**, 228-240.

19. J. I. Paredes, S. Villar-Rodil, A. Martínez-Alonso and J. M. D. Tascón, *Langmuir*, 2008, **24**, 10560-10564.

20. K. X. Yao, X. Liu, Z. Li, C. C. Li, H. C. Zeng and Y. Han, *ChemCatChem*, 2012, **4**, 1938-1942.

21. S. H. Joo, J. Y. Park, J. R. Renzas, D. R. Butcher, W. Huang and G. A. Somorjai, *Nano Letters*, 2010, **10**, 2709-2713.

22. B. Lin, K. Wei, J. Ni and J. Lin, *ChemCatChem*, 2013, **5**, 1941-1947.

23. M. Giovanni, H. L. Poh, A. Ambrosi, G. Zhao, Z. Sofer, F. Sanek, B. Khezri, R. D. Webster and M. Pumera, *Nanoscale*, 2012, **4**, 5002-5008.

24. L. Li, Z. H. Zhu, G. Q. Lu, Z. F. Yan and S. Z. Qiao, *Carbon*, 2007, **45**, 11-20.

25. L. Wang and R. T. Yang, *The Journal of Physical Chemistry C*, 2008, **112**, 12486-12494.

26. J. Bu, J.-L. Liu, X.-Y. Chen, J.-H. Zhuang, S.-R. Yan, M.-H. Qiao, H.-Y. He and K.-N. Fan, *Catalysis Communications*, 2008, **9**, 2612-2615.

27. M. F. F. Rodrigues and A. J. G. Cobo, *Catalysis Today*, 2010, **149**, 321-325.

28. A. Guerrero-Ruiz, P. Badenes and I. Rodríguez-Ramos, *Applied Catalysis A: General*, 1998, **173**, 313-321.

29. H.-G. Jung, Y. S. Jeong, J.-B. Park, Y.-K. Sun, B. Scrosati and Y. J. Lee, *ACS Nano*, 2013, **7**, 3532-3539.

30. N. Cao, W. Luo and G. Cheng, *International Journal of Hydrogen Energy*, 2013, **38**, 11964-11972.

31. D. Marquardt, C. Vollmer, R. Thomann, P. Steurer, R. Mülhaupt, E. Redel and C. Janiak, *Carbon*, 2011, **49**, 1326-1332.

32. W. Xiao, Z. Sun, S. Chen, H. Zhang, Y. Zhao, C. Huang and Z. Liu, *RSC Advances*, 2012, **2**, 8189-8193.

33. X. Liu, K. X. Yao, C. Meng and Y. Han, *Dalton Transactions*, 2012, **41**, 1289-1296.

34. Y. Zhou, Q. Bao, L. A. L. Tang, Y. Zhong and K. P. Loh, *Chemistry of Materials*, 2009, **21**, 2950-2956.

35. T. Adschiri, Y.-W. Lee, M. Goto and S. Takami, *Green Chemistry*, 2011, **13**, 1380-1390.

36. Z. Liu and B. Han, *Advanced Materials*, 2009, **21**, 825-829.

37. X.-R. Ye, Y. Lin, C. Wang, M. H. Engelhard, Y. Wang and C. M. Wai, *Journal of Materials Chemistry*, 2004, **14**, 908-913.

38. Y. Zhang and C. Erkey, *The Journal of supercritical fluids*, 2006, **38**, 252-267.

39. J. Zhao, L. Zhang, T. Chen, H. Yu, L. Zhang, H. Xue and H. Hu, *The Journal of Physical Chemistry C*, 2012, **116**, 21374-21381.

40. H. Hu, Y. Liu, Q. Wang, J. Zhao and Y. Liang, *Materials Letters*, 2011, **65**, 2582-2584.

41. J. Moulder, W. Stickle, P. Sobol and K. Bomben, 1992.

42. S. Miao, Z. Liu, B. Han, J. Huang, Z. Sun, J. Zhang and T. Jiang, *Angewandte Chemie International Edition*, 2006, **45**, 266-269.

43. R. Finke, Marcel Dekker: New York, 2002, pp. 17-54.

44. A. Roucoux, J. Schulz and H. Patin, *Chemical Reviews*, 2002, **102**, 3757-3778.

45. F. Su, L. Lv, F. Y. Lee, T. Liu, A. I. Cooper and X. S. Zhao, *Journal of the American Chemical Society*, 2007, **129**, 14213-14223.

46. J.-Y. Chang, A. Ghule, J.-J. Chang, S.-H. Tzing and Y.-C. Ling, *Chemical physics letters*, 2002, **363**, 583-590.

47. W. Chen, X. Pan and X. Bao, *Journal of the American Chemical Society*, 2007, **129**, 7421-7426.

48. D. Duca, F. Ferrante and G. La Manna, *The Journal of Physical Chemistry C*, 2007, **111**, 5402-5408.

49. X. Pan, Z. Fan, W. Chen, Y. Ding, H. Luo and X. Bao, *Nature materials*, 2007, **6**,

507-511.

50. S. Pei and H.-M. Cheng, *Carbon*, 2012, **50**, 3210-3228.

51. J. Martí, J. Sala and E. Guàrdia, *Journal of Molecular Liquids*, 2010, **153**, 72-78.